anatomia

MDPI

Article

Morphometric and Morphological Analysis of the Pulmonary Auscultatory Triangle in Human Fetuses: Anatomical Insights for Thoracic Surgery

Caio Siqueira Kuhn [1], Marcelo Lucas de Lima Prado [1], Iapunira Catarina Sant'Anna Aragão [2], Felipe Matheus Sant'Anna Aragão [3], Francisco Prado Reis [4], Deise Maria Furtado de Mendonça [5] and José Aderval Aragão [5,*]

1 Department of Medicine, Federal University of Sergipe (UFS), Aracaju 49060-100, SE, Brazil; caioskuhn10@hotmail.com (C.S.K.); marcelolucas953@gmail.com (M.L.d.L.P.)
2 Munir Rafful Municipal Hospital (MHMR), Volta Redonda 27277-130, RJ, Brazil; icatarinasaragao@hotmail.com
3 Heart Institute of the Hospital das Clínicas, Faculty of Medicine, University of São Paulo (INCOR), São Paulo 05403-900, SP, Brazil; felipemsaragao@hotmail.com
4 Medical School, Tiradentes University (UNIT), Aracaju 49032-490, SE, Brazil; franciscopradoreis@gmail.com
5 Department of Morphology, Federal University of Sergipe (UFS), São Cristóvão 49100-000, SE, Brazil; deisemfmendonca@gmail.com
* Correspondence: adervalufs@gmail.com

Abstract

Objectives: The Pulmonary Auscultatory Triangle (PAT) is a bilateral region on the back delimited by the trapezius, latissimus dorsi, and scapula. Beyond its relevance for pulmonary auscultation, PAT also represents an important anatomical window for posterior thoracic approaches. While its anatomy has been extensively described in adults, data on its developmental morphology during fetal life remain scarce. This original morphometric study aimed to characterize the morphometry and morphology of the PAT in human fetuses and to evaluate differences according to sex, side, and gestational age. Methods: A total of 80 PATs from 40 human fetuses (20 male and 20 female) were examined. Using ImageJ software 1.54k, we measured margin lengths (inferior trapezius, medial scapular, and superior latissimus), area, and perimeter. Morphological classification was performed based on internal angles. Associations with sex, side, and gestational age were statistically assessed. Results: The mean gestational age was 28.6 weeks. PAT had a mean area of 103.2 mm^2 and a mean perimeter of 49.1 mm. Mean margin lengths were 20.1 mm for the trapezius, 12.4 mm for the scapular margin, and 16.6 mm for the latissimus dorsi. Three morphologies were observed: acute (42.5%), obtuse (25.0%), and rectangular (32.5%). A significant asymmetry in shape distribution was found between sides ($p = 0.034$). Weak but statistically significant positive correlations with gestational age were found for perimeter and for the trapezius and latissimus dorsi margins, indicating progressive enlargement with fetal growth. Conclusions: This study provides the first detailed morphometric and morphological description of the PAT in human fetuses. The findings establish a developmental anatomical baseline for the posterior thoracic wall and highlight growth-related changes and side-related variability.

Keywords: thoracic wall; surgical anatomy; fetal thoracic morphology; minimally invasive techniques; thoracic muscles

Academic Editor: Francesco Fornai

Received: 19 November 2025
Revised: 25 January 2026
Accepted: 31 January 2026
Published: 9 February 2026

1. Introduction

The Pulmonary Auscultatory Triangle (PAT) is a bilateral triangular region on the dorsal surface, bounded by the inferior margin of the trapezius muscle, the superior margin of the latissimus dorsi muscle, and the medial border of the scapula. Its floor is formed by the rhomboid major muscle and, occasionally, by the erector spinae muscle. However, the literature shows inconsistencies regarding its precise boundaries [1].

The PAT occupies a strategically important region on the posterior thoracic wall. It overlies the inferior pulmonary lobe and its segments, thereby enhancing posterior auscultation sensitivity. In addition, it serves as a key anatomical landmark for pulmonary auscultation and posterior thoracic access [2,3]. Its clinical relevance extends to surgical practice, particularly because posterior or posterolateral approaches through the PAT allow access to thoracic structures while preserving major muscles. This muscle-sparing characteristic underlies its classification as a minimally invasive approach, associated with reduced tissue trauma and favorable postoperative outcomes [4–14]. Given these anatomical and clinical implications, a detailed morphometric characterization of the PAT is essential to support safer and more precise clinical and surgical interventions [13–16].

Although the clinical relevance of the PAT is well established in adult thoracic examination, surgery, and regional anesthesia, its developmental anatomy during the fetal period remains poorly characterized. Most available studies addressing thoracic anatomy in fetuses focus on lung development, thoracic dimensions, or other anatomical landmarks, with little attention given to the morphometric configuration of the PAT. To date, detailed fetal morphometric data on the PAT are scarce, and its developmental variability, symmetry, and dimensional relationships during gestation are largely unexplored. Understanding fetal PAT morphometry is relevant not only from a developmental anatomy perspective but also as a baseline for postnatal anatomical maturation and future translational studies correlating fetal, neonatal, and pediatric thoracic anatomy. In this context, the present study provides an original morphometric analysis of the fetal PAT, aiming to fill this gap by systematically characterizing its dimensions and morphology, considering sex, side, and gestational age. and side-related differences.

2. Materials and Methods

Sample.

Morphometric and morphological analysis was performed on a total of 80 PATs (Figure 1), obtained from 40 human fetuses from the Anatomy Laboratory of the Morphology Department, Federal University of Sergipe. The sample comprised 20 male and 20 female fetuses. Inclusion criteria included fetuses with well-preserved dorsal anatomy with intact lower limbs. Fetuses presenting congenital defects of the posterior thoracic wall, such as myelomeningocele or spina bifida, or with other macroscopic alterations of the dorsum, were excluded. Fetuses lacking lower limbs were also excluded.

The triangle is bordered superiorly by the trapezius muscle (T), laterally by the scapula (S), and inferiorly by the latissimus dorsi muscle (LD). The floor is formed by the rhomboid major muscle (RM).

Ethical Statement.

The study was conducted in accordance with the ethical principles outlined in the Declaration of Helsinki and complied with institutional and national regulations governing the ethical use of human cadaveric material for research and educational purposes. In Brazil, Law No. 8.501, enacted on 30 November 1992, regulates the donation of unclaimed bodies by public hospitals (fetuses) or forensic medical institutes to universities for teaching and scientific research purposes. In such cases, the requirement for informed consent is waived, as the law provides the legal framework for the ethical use of unclaimed cadaveric material in academic and scientific contexts.

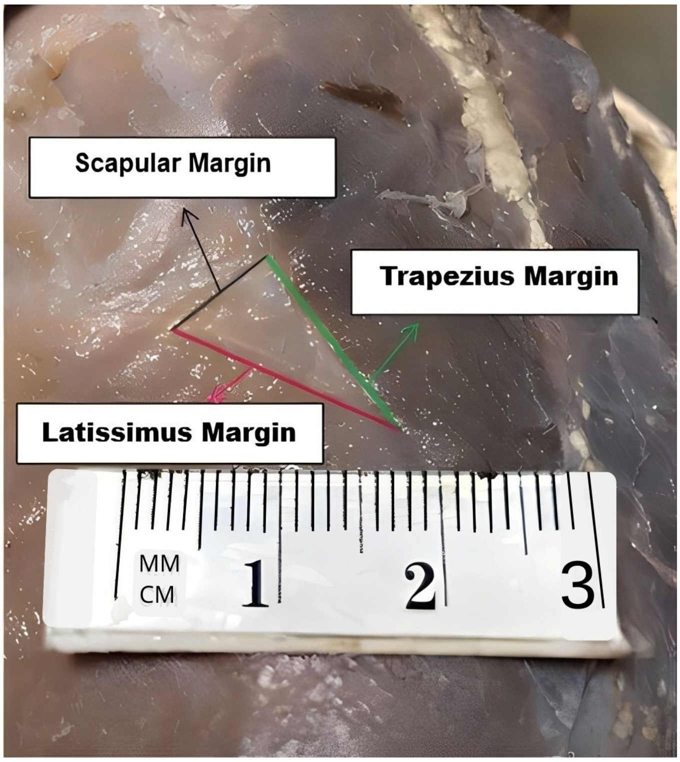

Figure 1. Posterior view of the thoracic region showing the anatomical limits of the PAT.

Determination of Gestational Age.

A non-probability convenience sampling method was applied. Fetal ages were calculated using the formula derived from Goldstein's studies [17] (Gestational Age = 8.2982 + 0.38764 × Fetal Foot Length). Hallux–calcaneal length was measured with a digital caliper (0.01 mm precision).

Dissection and Photographic Documentation.

After dissection of the dorsum, focusing on the triangle region, photographs were taken. A ruler was included in each image to provide a scale for accurate measurements with ImageJ software. This allowed precise delimitation of the PAT (Figure 2) and measurement of its margins (inferior trapezius, medial scapular, and superior latissimus).

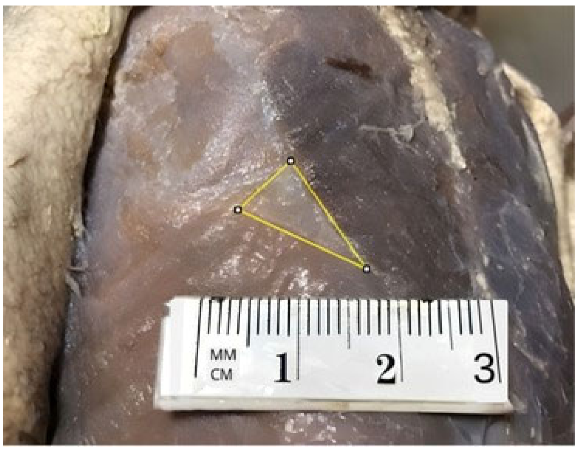

Figure 2. Precise delimitation of the Pulmonary Auscultatory Triangle margins in human fetuses using ImageJ software.

Triangle Delimitation and Measurements.

In addition to measuring the margins of the muscles, the area, perimeter, and morphological shape of the PAT (Figure 3) were also determined. PATs were classified as acute triangles (angles < 85°), obtuse triangles (one angle > 95°), or right-angled triangles (approximately 90°, ±5° tolerance). Data were organized in a spreadsheet for statistical analysis, focusing on correlations between measurements and the variables of age, sex, and side.

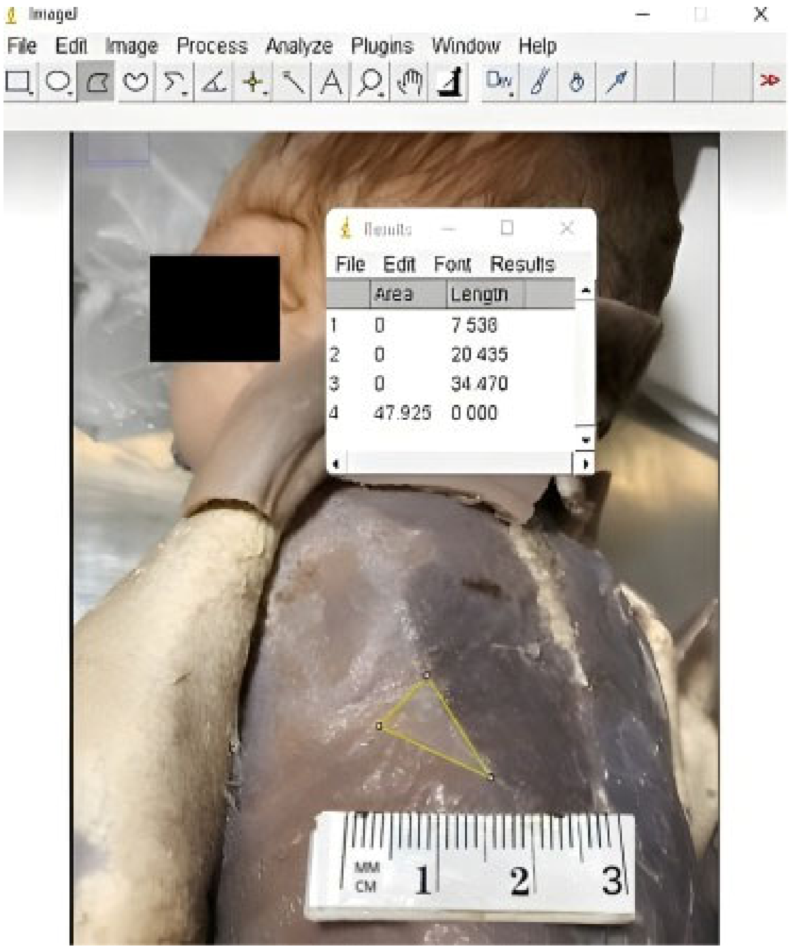

Figure 3. Morphometric analysis of the Pulmonary Auscultatory Triangle with ImageJ: measurement of margins, perimeter, and area. (1) Scapular margin length; (2) Sum of scapular margin length and trapezius margin length; (3) Perimeter; (4) Area.

Intra-observer reliability.

All ImageJ tracings and morphometric measurements were performed by a single trained observer to ensure methodological consistency, following a standardized measurement protocol. To assess intra-observer reliability, a randomly selected subset of 20% of the images (no. = 16) was reanalyzed by the same observer after a 15-day interval under blinded conditions. Measurement repeatability was quantified using the Intraclass Correlation Coefficient (ICC), adopting a two-way random-effects model with absolute agreement for a single rater (ICC 2,1). In addition, the Technical Error of Measurement (TEM) and the relative Technical Error of Measurement (rTEM) were calculated to provide complementary estimates of absolute and relative measurement precision.

Photographic Acquisition and Standardization.

Photographic documentation was performed using a digital camera, with images acquired at high resolution to ensure clear visualization of anatomical landmarks. The distance between the camera and the specimen was kept constant across all acquisitions.

Uniform lighting conditions were applied to reduce shadows and reflections. A metric scale was included in all images to allow spatial calibration during subsequent ImageJ analysis. This standardized photographic protocol was adopted to optimize measurement accuracy and reproducibility.

Statistical Analysis.

Descriptive statistics were applied to summarize the variables, including mean, median, standard deviation, interquartile range, and absolute and relative frequencies. The Chi-square test was employed to investigate the association between different categorical variables, allowing for the assessment of whether observed frequencies differed from expected frequencies, thereby indicating potential statistically significant associations between the variables [18]. Normality of the quantitative data was assessed using the Shapiro–Wilk test [19]. As the data did not follow a normal distribution, non-parametric methods were adopted. Specifically, the Wilcoxon–Mann–Whitney test was applied to compare medians between two independent groups [20], and Spearman's rank correlation coefficient was used to assess the strength and direction of associations between continuous variables [21]. Confidence intervals (95%) were calculated for Spearman correlation coefficients to provide estimates of precision.

All statistical analyses were performed in the R environment (version 4.3.2) [22], with the significance level set at 5% ($p < 0.05$).

A priori sample size calculation or power analysis was not performed, as the study was based on the availability of fetal specimens meeting strict inclusion criteria. This approach is consistent with exploratory descriptive studies in developmental anatomy.

To facilitate interpretation, statistically significant findings are explicitly highlighted in the text, while complete numerical data are provided in the tables.

3. Results

Intra-observer reliability.

The numerical results of the intra-observer reliability analysis are presented in Table 1. The intraclass correlation coefficients (ICC 2,1) ranged from 0.967 to 0.986 across all morphometric variables, indicating excellent measurement repeatability. Additionally, the relative Technical Error of Measurement (rTEM) ranged from 3.48% to 5.54%, demonstrating low measurement error in relation to the biological variability of the sample and supporting the robustness of the morphometric protocol.

Table 1. Intra-observer reliability and measurement error indices for the morphometric variables of the PAT.

Characteristics	ICC (2, 1) [95% CI]	TEM (abs)	rTEM (%)	*p*-Value
Triangle Area (mm^2)	0.982 [0.950; 0.994]	4.572	5.54%	<0.001
Perimeter of Triangle (mm)	0.970 [0.915; 0.989]	1.800	4.04%	<0.001
Trapezius Triangle Margin Length (mm)	0.967 [0.910; 0.988]	0.858	4.78%	<0.001
Scapula Triangle Margin Length (mm)	0.969 [0.914; 0.989]	0.379	3.51%	<0.001
Latissimus Triangle Margin Length (mm)	0.986 [0.960; 0.995]	0.551	3.48%	<0.001

Note: ICC (2, 1) = Intraclass Correlation Coefficient (two-way random effects, absolute agreement, single rater model); 95% CI = 95% confidence interval; TEM (abs) = absolute Technical Error of Measurement, calculated as TEM = $\sqrt{(\Sigma d^2/2n)}$; rTEM (%) = relative Technical Error of Measurement, calculated as (TEM/grand mean) × 100; *p*-value = statistical significance of the ICC. ICC values > 0.90 indicate excellent reliability, and rTEM values < 5.0% indicate high measurement precision in morphometric studies.

Sample Characteristics.

The mean gestational age of the fetuses was 28.6 ± 3.5 weeks, with a median of 28.2 weeks (IQR: 26.0–31.0). The mean area of the PAT was 103.2 ± 52.1 mm^2 (median: 97.7 mm^2; IQR: 67.1–123.0), and the mean perimeter was 49.1 ± 12.0 mm (median: 49.3 mm; IQR: 40.4–55.3).

General Morphometry and Morphological Classification of the PAT.

The trapezius margin measured 20.1 ± 5.2 mm, with a median of 20.3 mm (IQR: 16.1–22.8). The scapular margin measured 12.4 ± 3.2 mm, with a median of 12.1 mm (IQR: 10.4–13.8). The latissimus dorsi margin measured 16.6 ± 4.9 mm, with a median of 16.7 mm (IQR: 13.0–18.9). Regarding morphology, 42.5% of the triangles were classified as acute, 25.0% as obtuse, and 32.5% as rectangular (Figure 4).

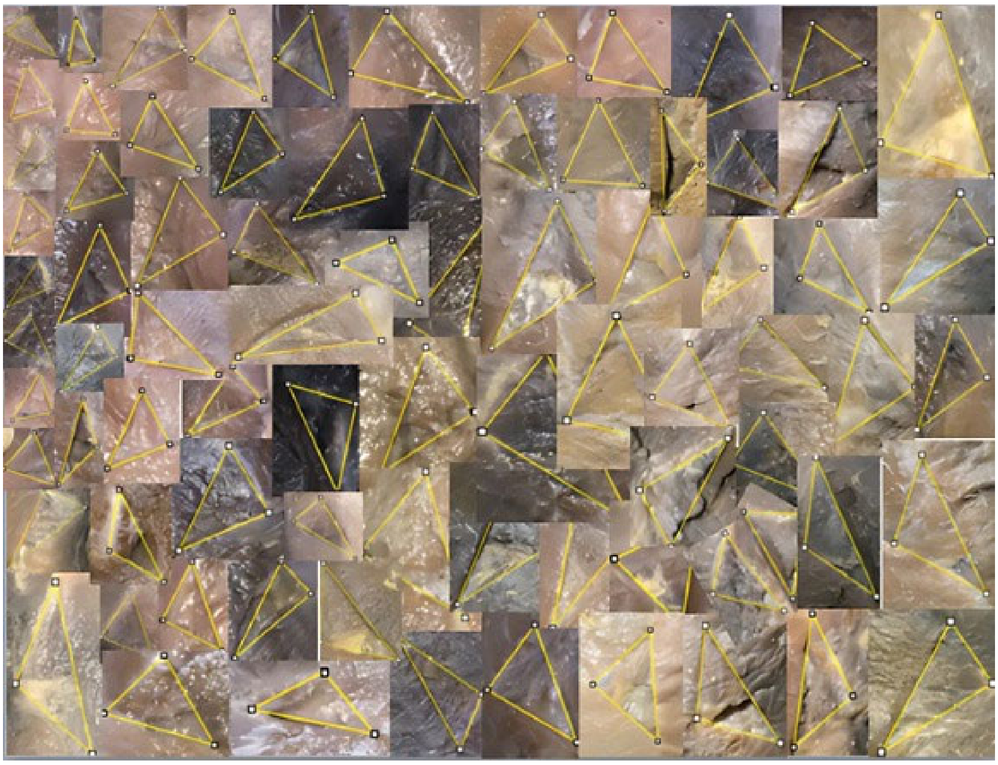

Figure 4. Mosaic of PAT Shapes obtained from the dissection of 40 human fetuses (80 PATs in total, right and left sides). The images illustrate the morphological variability of the triangles, which were classified as acute, obtuse, or approximately right-angled based on their internal angles. This panel provides a comprehensive visual representation of the range of anatomical presentations observed in the sample.

Sex-Related Comparisons.

Regarding sex, the mean gestational age was 28.9 ± 3.2 weeks for female fetuses and 28.4 ± 3.8 weeks for male fetuses. The median age was 29.6 weeks (IQR: 25.8–31.1) for females and 27.5 weeks (IQR: 26.1–30.8) for males. No significant difference was found between groups (p = 0.410).

The mean area was 97.6 ± 36.8 mm^2 in females and 108.9 ± 63.9 mm^2 in males. The medians were nearly identical (97.7 mm^2 vs. 98.0 mm^2), with overlapping IQRs and no significant sex-related difference (p = 0.684).

The mean perimeter was 48.7 ± 9.7 mm in females and 49.5 ± 14.0 mm in males, with medians of 49.7 and 49.3 mm, respectively. The IQRs were similar, and no significant difference was observed (p = 0.973).

The trapezius margin measured 20.2 ± 4.4 mm in females and 20.1 ± 6.0 mm in males, without statistically significant differences (p = 0.785). The scapular margin measured

https://doi.org/10.3390/anatomia5010005

12.1 ± 2.6 mm in females and 12.8 ± 3.7 mm in males, also without significant difference ($p = 0.303$). The latissimus margin measured 16.5 ± 4.1 mm in females and 16.7 ± 5.7 mm in males, with no significant difference ($p > 0.999$).

Regarding morphology, no sex-related differences were observed ($p = 0.298$) (Table 2). Detailed morphometric values by sex and side are summarized in Tables 2 and 3.

Table 2. Correlation of the Triangle with Sex.

		Sex		
Characteristics	**Total, N = 80**	**Female, N = 40**	**Male, N = 40**	***p* Value**
Age				
Mean (Standard Deviation)	28.6 (3.5)	28.9 (3.2)	28.4 (3.8)	0.410 [1]
Median [IA]	28.2 [26.0, 31.0]	29.6 [25.8, 31.1]	27.5 [26.1, 30.8]	
Side, n/(%)				
Right	40/(50.0%)	20/(50.0%)	20/(50.0%)	>0.999 [2]
Left	40/(50.0%)	20/(50.0%)	20/(50.0%)	
Triangle Area (mm^2)				
Mean (Standard Deviation)	103.2 (52.1)	97.6 (36.8)	108.9 (63.9)	0.684 [3]
Median [IQR]	97.7 [67.1, 123.0]	97.7 [66.8, 110.4]	98.0 [70.1, 135.7]	
Perimeter of Triangle (mm)				
Mean (Standard Deviation)	49.1 (12.0)	48.7 (9.7)	49.5 (14.0)	0.973 [3]
Median [IQR]	49.3 [40.4, 55.3]	49.7 [41.6, 54.0]	49.3 [39.4, 55.8]	
Trapezius Triangle Margin Length (mm)				
Mean (Standard Deviation)	20.1 (5.2)	20.2 (4.4)	20.1 (6.0)	0.785 [3]
Median [IQR]	20.3 [16.1, 22.8]	20.6 [17.1, 22.1]	20.1 [15.2, 22.9]	
Scapula Triangle Margin Length (mm)				
Mean (Standard Deviation)	12.4 (3.2)	12.1 (2.6)	12.8 (3.7)	0.303 [1]
Median [IQR]	12.1 [10.4, 13.8]	11.5 [10.2, 13.3]	12.6 [10.6, 14.2]	
Latissimus Triangle Margin Length (mm)				
Mean (Standard Deviation)	16.6 (4.9)	16.5 (4.1)	16.7 (5.7)	>0.999 [1]
Median [IQR]	16.7 [13.0, 18.9]	16.8 [13.0, 18.5]	16.3 [13.3, 19.5]	
Triangle Morphology, n/(%)				
Acute	34/(42.5%)	15/(37.5%)	19/(47.5%)	0.298 [2]
Obtuse	20/(25.0%)	13/(32.5%)	7/(17.5%)	
Rectangle	26/(32.5%)	12/(30.0%)	14/(35.0%)	

[1] Wilcoxon rank sum test. [2] Chi-square test of independence. [3] Wilcoxon rank sum exact test. Legend: n—Absolute frequency. N—Valid data. %—Percentage. SD—Standard Deviation. IQR—Interquartile Range.

Table 3. Correlation of the Triangle with Side.

	Side		
Characteristics	**Right, N = 40**	**Left, N = 40**	***p* Value**
Age			
Mean (Standard Deviation)	28.6 (3.5)	28.6 (3.5)	>0.9991
Median [IQR]	28.2 [26, 31]	28.2 [26, 31]	
Triangle Area (mm^2)			
Mean (Standard Deviation)	98 (43)	108 (60)	0.852 [2]
Median [IQR]	102.1 [66.4, 113.4]	93.7 [68.4, 135.7]	

Table 3. *Cont.*

	Side		
Characteristics	**Right, N = 40**	**Left, N = 40**	***p* Value**
Triangle Perimeter (mm)			
Mean (Standard Deviation)	48.7 (11)	49.5 (13)	0.807 [2]
Median [IQR]	50.6 [41.7, 54.3]	47.2 [39.7, 56.9]	
Trapezius Triangle Margin Length (mm)			
Mean (Standard Deviation)	20.2 (4.6)	20 (5.8)	0.424 [2]
Median [IQR]	20.7 [16.6, 22.9]	19 [15.7, 22.5]	
Latissimus Triangle Margin Length (mm)			
Mean (Standard Deviation)	16.6 (5.2)	16.5 (4.7)	0.777 [1]
Median [IQR]	17.3 [13.3, 18.6]	16 [13, 19.1]	
Triangle Morphology, n/(%)			
Acute	12/(30%)	22/(55%)	0.034 [3]
Obtuse	10/(25%)	10/(25%)	
Rectangular	18/(45%)	8/(20%)	

[1] Wilcoxon rank sum test. [2] Wilcoxon rank sum exact test. [3] Chi-square test of independence. Legend: n—Absolute frequency, N—Valid data, %—Percentage, SD—Standard Deviation, IQR—Interquartile Range.

Side-Related Comparisons (Right vs. Left).

Comparing sides, the mean area was 98.5 ± 43.0 mm^2 for right-sided triangles and 108.0 ± 60.0 mm^2 for left-sided triangles. The medians were 102.1 mm^2 for the right side and 93.7 mm^2 for the left side, with overlapping IQRs and no significant difference (p = 0.852).

The mean perimeter was 48.7 ± 11.0 mm on the right and 49.5 ± 13.0 mm on the left. The medians were 50.6 and 47.2 mm, respectively, with similar IQRs and no significant difference (p = 0.807).

The trapezius margin measured 20.2 ± 4.6 mm on the right and 20.0 ± 5.8 mm on the left, with medians of 20.7 and 19.0 mm, respectively, showing no statistically significant difference (p = 0.424). The scapular margin measured 11.9 ± 2.6 mm on the right and 13.0 ± 3.6 mm on the left, with medians of 11.7 and 12.3 mm, respectively, with no statistically significant difference (p = 0.172). The latissimus dorsi margin was similar on both sides, measuring 16.6 ± 5.2 mm on the right and 16.5 ± 4.7 mm on the left, with medians of 17.3 and 16.0 mm, respectively, also with no statistically significant difference (p = 0.777).

A statistically significant asymmetry in PAT morphology was observed between sides (p = 0.034), with acute configurations predominating on the left side (55.0%) and rectangular configurations more frequent on the right side (45.0%) (Table 3).

Correlation with Gestational Age.

Gestational age showed significant positive correlations with several morphometric parameters. The strongest association was observed for the trapezius margin length (R = 0.31, p = 0.005), followed by the triangle perimeter (R = 0.29, p = 0.009) and latissimus dorsi margin length (R = 0.22, p = 0.048). These findings indicate progressive enlargement of specific PAT dimensions with advancing fetal age (Figure 5).

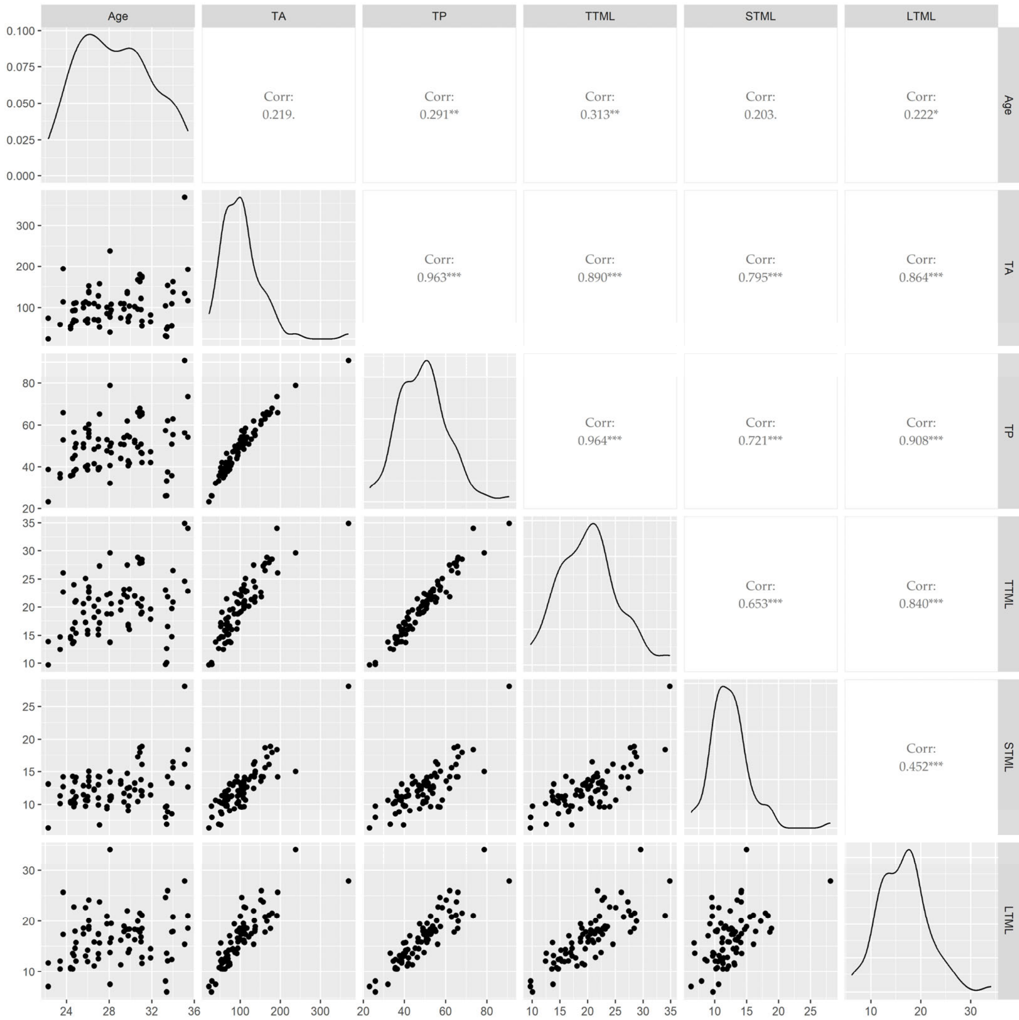

Figure 5. Scatter plots show the correlation between gestational age and the morphometric parameters of the PAT. Each point represents a single PAT measurement. Regression lines are included to illustrate trends. Significant positive correlations were observed for the perimeter (R = 0.29; $p = 0.009$), trapezius margin length (R = 0.31; $p = 0.005$), and latissimus dorsi margin length (R = 0.22; $p = 0.048$). No significant correlations were found for the area (R = 0.22; $p = 0.051$) or scapular margin length (R = 0.20; $p = 0.071$). TA—Triangle Area, TP—Triangle Perimeter, TTML—Trapezius Triangle Margin Length, STML—Scapula Triangle Margin Length, LTML—Latissimus Triangle Margin Length.

4. Discussion

Developmental Anatomy of the PAT in Fetuses.

The PAT represents a triangular region defined by the spatial relationship between the trapezius muscle, latissimus dorsi muscle, scapula, and underlying thoracic wall. In fetuses, these anatomical structures are subject to continuous growth, positional remodeling, and proportional changes throughout gestation. Unlike adult anatomy, fetal musculoskeletal organization is characterized by ongoing migration of muscle insertions, scapular rotation, and progressive expansion of the posterior thoracic wall [15,17]. Consequently, variability in both the size and morphology of the PAT during fetal life is expected and reflects normal developmental dynamics rather than fixed anatomical configurations.

The present study contributes to the literature by providing one of the first detailed morphometric characterizations of the PAT in human fetuses. Most previous investigations have focused on adult surgical anatomy or clinical applications such as auscultation and thoracic interventions, leaving a gap in knowledge regarding the prenatal morphology of this region [4–14]. By documenting fetal PAT dimensions and shapes, this study establishes a developmental baseline that may inform future anatomical, imaging, and clinical research.

Clinical Significance and Surgical Implications.

Such knowledge may facilitate pulmonary auscultation for clinicians and assist surgeons in selecting optimal approaches during procedures involving this region. Surgical approaches through the PAT typically employ a posterior or posterolateral incision [13]. This approach avoids the division of muscles such as the latissimus dorsi, serratus anterior, and trapezius, thereby rendering it minimally invasive [8,15]. This access provides wide exposure to posterior, lateral, and subscapular fractures [5], as well as excellent exposure of the pleura, thoracic cavity, and posterior mediastinum [8]. Because ribs from the third to the seventh are the most frequently fractured, given their exposed anatomical position, they are particularly susceptible to injury [23]. Fractures extending to the second posterior rib can also be reached via a PAT incision, which offers a strategic advantage by creating a horizontal, tunnel-like space that ensures complete visualization of the fracture [23]. Such exposure can often be achieved with minimal retraction of the PAT's muscular borders using percutaneous and right-angle instruments [5]. In cases of thoracic trauma with associated rib fractures, internal fixation through the PAT has proven more effective than external fixation, with benefits including lower surgical site infection rates, faster wound healing, reduced wound dehiscence, shorter hospital stays, and quicker recovery [23]. However, it is worth noting that more cephalic or caudal fractures may still necessitate partial or complete division of overlying muscles during PAT access [5]. Standard posterolateral muscle-cutting thoracotomies in pediatric patients are associated with morbidities in terms of unsatisfactory motor and aesthetic outcomes and a greater need for postoperative analgesia when compared to the muscle-preserving technique [24].

Overall, PAT-based offers less postoperative pain, improved shoulder function, and earlier hospital discharge [10], with low bleeding and excellent exposure for repairs, reducing delayed healing, residual muscle weakness and wound dehiscence [8].

PAT anatomy and contemporary regional anesthesia applications.

Beyond its traditional surgical applications, the PAT has gained renewed clinical relevance in contemporary regional anesthesia. Recent studies have described the use of the triangle of auscultation as a key anatomical landmark for rhomboid intercostal and rhomboid intercostal-subserratus plane blocks, which provide effective analgesia for thoracic surgery, rib fractures, and thoracic wall pain. These ultrasound-guided techniques rely on precise anatomical relationships between the rhomboid major muscle, intercostal spaces, and underlying thoracic structures, reinforcing the importance of detailed morphometric knowledge of this region [25–27]. Although these applications have been described in adult populations, the present fetal morphometric findings contribute to a foundational anatomical understanding that may inform future investigations into the developmental anatomy underlying such regional anesthetic approaches.

Morphological Variability and Left–Right Asymmetry.

Morphological analysis revealed substantial variability in PAT shape, with acute, obtuse, and approximately right-angled configurations observed across the sample. A statistically significant asymmetry was identified between sides, with acute shapes more frequently observed on the left and rectangular shapes predominating on the right. This asymmetry may be influenced by multiple factors.

From a biological perspective, subtle left–right differences in scapular positioning, asymmetric growth of thoracic organs, or inherent developmental asymmetry may contribute to these findings. Alternatively, technical factors such as fetal positioning during preservation, fixation-related tissue deformation, or dissection handling may have affected the apparent morphology. Because fetal orientation and post-mortem handling were not systematically controlled, the observed asymmetry should be interpreted cautiously. Future studies incorporating imaging-based assessments or standardized positioning protocols may help distinguish true developmental asymmetry from methodological influences.

Morphometric Growth Patterns and Gestational Age Correlations.

The observed positive correlations between gestational age and specific PAT parameters, particularly the trapezius margin length, latissimus dorsi margin length, and overall triangle perimeter, are consistent with progressive musculoskeletal growth of the posterior thoracic region. These associations likely reflect coordinated enlargement of the scapula and surrounding musculature rather than isolated expansion of the triangle itself. The absence of a statistically significant correlation between gestational age and triangle area suggests that proportional growth may occur non-uniformly across the triangle's margins during fetal development.

These findings highlight that the PAT is a dynamic anatomical region during gestation, undergoing gradual dimensional changes that parallel overall thoracic growth. Such developmental patterns should be considered when interpreting fetal thoracic anatomy and underscore the importance of age-specific morphometric data.

Clinical Relevance and Translational Considerations.

Although the PAT is widely recognized in adult anatomy for its role in pulmonary auscultation, thoracic surgery, and regional anesthesia techniques, direct clinical translation of fetal morphometric data requires careful consideration. Fetal anatomy differs substantially from neonatal and pediatric anatomy in terms of absolute size, tissue composition, rib orientation, and musculoskeletal proportions. Therefore, the present findings should not be directly extrapolated to surgical practice without acknowledging these developmental differences.

Nevertheless, fetal morphometric data provide valuable foundational information that can support future translational research. Establishing normative developmental patterns of the PAT may aid in correlating prenatal anatomy with postnatal imaging, neonatal anatomy, and pediatric surgical landmarks. Within this context, the consistently high intra-observer reliability achieved across all measurements in this study reinforces the methodological rigor of the study and substantiates the reliability of the reported morphometric data. As such, these data provide a robust anatomical foundation for future translational and developmental investigations. Further studies integrating fetal imaging, neonatal dissections, and longitudinal growth analyses are needed to clarify how fetal PAT morphology scales into infancy and childhood.

5. Conclusions

This study provides one of the first detailed morphometric and morphological characterizations of the PAT during fetal development, addressing a relevant gap in developmental thoracic anatomy. The results demonstrate that PAT dimensions and morphology vary with gestational age and exhibit side-related differences, reflecting the dynamic growth of the posterior thoracic wall.

These findings should be interpreted considering the study's limitations, including the use of fetal specimens from a single population and potential influences of post-mortem preservation. Moreover, because fetal anatomy differs substantially from neonatal and pediatric anatomy, direct clinical translation requires caution.

Despite these constraints, the present data establishes a valuable developmental anatomical reference that may inform future prenatal imaging studies, neonatal anatomical investigations, and longitudinal research exploring how fetal thoracic anatomy evolves into postnatal life. Such efforts may ultimately refine anatomical orientation and contribute to safer and more precise applications involving the posterior thoracic region.

https://doi.org/10.3390/anatomia5010005

Author Contributions: Formal analysis, Writing—original draft: C.S.K. and M.L.d.L.P. Methodology and investigation: I.C.S.A. and F.M.S.A. Writing—review and editing: D.M.F.d.M. and F.P.R. Project administration, Writing—review: J.A.A. All authors have read and agreed to the published version of the manuscript.

Funding: This research received no external funding.

Institutional Review Board Statement: This study was conducted in accordance with the ethical principles of the Declaration of Helsinki and complied with institutional and national regulations governing the use of human cadaveric material for research and education. In Brazil, Law No. 8.501 (30 November 1992) authorizes public universities to receive unclaimed human bodies, including fetuses, from public hospitals or forensic institutes for scientific and educational purposes. Under the authors' responsibility, and in accordance with the provisions of Law No. 8.501 (30 November 1992), this study did not require specific approval from an Ethics Committee.

Informed Consent Statement: Not applicable.

Data Availability Statement: All original contributions of this study are contained within the article, and further information is available from the corresponding author upon request.

Acknowledgments: We thank Marcelo Diaz Nascimento, Gladson Gomes de Souza, and Luís Henrique Santos Fortes, anatomy laboratory technicians at the Federal University of Sergipe, for their support in preparing the cadavers, since without their collaboration, this work could not have been accomplished. The authors wish to sincerely thank those who donated their bodies to science so that anatomical research could be carried out. The results of this research can potentially improve patient care and increase the overall knowledge of humanity. Therefore, these donors and their families deserve our utmost gratitude. The authors have reviewed and edited the manuscript and take full responsibility for the content of this publication.

Conflicts of Interest: The authors declare no conflicts of interest.

Abbreviations

The following abbreviations are used in this manuscript:

TA	Triangle Area
TP	Triangle Perimeter
TTML	Trapezius Triangle Margin Length
STML	Scapula Triangle Margin Length
LTML	Latissimus Triangle Margin Length

References

1. Malik, N.; Tedder, B.L.; Zemaitis, M.R. Anatomy, Thorax, Triangle of Auscultation. In *StatPearls [Internet]*; StatPearls Publishing: Treasure Island, FL, USA, 2025. Available online: https://www.ncbi.nlm.nih.gov/books/NBK539958/ (accessed on 17 November 2025).
2. Gurgel, K.A.N.; Cerqueira, G.S.; Fontenele, A.C.; Vasconcelos, F.; Moura, J.R.S. Aspectos anatomoclínicos do trígono da ausculta: Um review. *Encontros Univ. UFC* **2019**, *4*, 2986.
3. DiDio, L.J.; Yeasting, R.A. Projection of the triangle of auscultation on the human pulmonary surface. *Int Surg.* **1977**, *62*, 338–340. [PubMed]
4. White, T.W.; Majercik, S. Rib Fracture Repair. *Shanghai Chest* **2017**, *1*, 11. [CrossRef]
5. Greiffenstein, P.; Tran, M.Q.; Campeau, L. Three common exposures of the chest wall for rib fixation: Anatomical considerations. *J. Thorac. Dis.* **2019**, *11*, S1034–S1043. [CrossRef]
6. Lau, O.J.; Shawkat, S. Pleurectomy through the triangle of auscultation. *Thorax* **1982**, *37*, 945–946. [CrossRef]
7. Prakash, S.; Kalra, P.; Khan, Y.; Dhal, A. Ventral scapular osteochondroma excision through "triangle of auscultation": A case series. *J. Orthop. Surg.* **2020**, *28*, 2309499019892848. [CrossRef]
8. Goh, D.W.; Brereton, R.J. Triangle of auscultation thoracotomy for esophageal atresia. *J. Thorac. Cardiovasc. Surg.* **1992**, *103*, 14–16. [CrossRef]

9. Horowitz, M.D.; Ancalmo, N.; Ochsner, J.L. Thoracotomy through the auscultatory triangle. *Ann. Thorac. Surg.* **1989**, *47*, 782–783. [CrossRef]
10. Nosotti, M.; Cioffi, U.; De Simone, M.; Rosso, L.; Mendogni, P.; Santambrogio, L. Muscle sparing versus posterolateral thoracotomy for pulmonary lobectomy: Randomised controlled trial. *Interact. Cardiovasc. Thorac. Surg.* **2010**, *11*, 415–419. [CrossRef]
11. Stamenovic, D.; Bostanci, K.; Messerschmidt, A. Posterior uniportal video-assisted thoracoscopic surgery for anatomical lung resections. *J. Thorac. Dis.* **2017**, *9*, 5261–5266. [CrossRef]
12. Stamenovic, D.; Messerschmidt, A. Posterior uniportal video-assisted thoracoscopic surgery for resection of the apical segment of the right lower lobe followed by completion lobectomy. *Interact. Cardiovasc. Thorac. Surg.* **2017**, *24*, 644–645. [CrossRef]
13. Caronia, F.P.; Arrigo, E.; Fiorelli, A. Uniportal video-assisted lobectomy through a posterior approach. *J. Thorac. Dis.* **2017**, *9*, 4057–4063. [CrossRef] [PubMed]
14. Gimferrer, J.M.; Belda, J.; Catalán, M.; Serra, M.; Rubio, M.; Iglesias, M. Lobectomía videoasistida a través del triángulo auscultatorio en el tratamiento quirúrgico del carcinoma broncopulmonar. Experiencia preliminar [Video-assisted lobectomy through the auscultatory triangle for the surgical treatment of bronchopulmonary carcinoma. Preliminary experience]. *Arch. Bronconeumol.* **2003**, *39*, 87–90. (In Spanish) [CrossRef]
15. Lee, L.; Lauzar, D.; Navarro, R.A. Minimally invasive thoracic surgery in children. *Semin. Pediatr. Surg.* **2007**, *16*, 14–23.
16. Jiménez, M.; Recalde, O.; Eufracio, O.; Alonso, C. Lobectomía por triángulo de auscultación en pediatría. *Cir. Pediatr.* **1992**, *5*, 187–190.
17. Goldstein, I. Growth of the fetal long bones and fetal age assessment. *J. Clin. Ultrasound* **1976**, *4*, 321–327.
18. Turhan, N.S. Karl pearson's chi-square tests. *Educ. Res. Rev.* **2020**, *16*, 575–580.
19. De Souza, R.R.; Toebe, M.; Mello, A.C.; Bittencourt, K.C. Sample size and shapiro-wilk test: An analysis for soybean grain yield. *Eur. J. Agron.* **2023**, *142*, 126666. [CrossRef]
20. Oti, E.U.; Olusola, M.O.; Esemokumo, P.A. Statistical analysis of the median test and the mann-whitney u test. *Int. J. Adv. Acad. Res.* **2021**, *7*, 44–51.
21. Alsaqr, A.M. Remarks on the use of Pearson's and Spearman's correlation coefficients in assessing relationships in ophthalmic data. *Afr. Vision Eye Health* **2021**, *80*, 10. [CrossRef]
22. R Core Team. R: A Language and Environment for Statistical Computing; R Foundation for Statistical Computing: Vienna, Austria. 2023. Available online: https://www.R-project.org/ (accessed on 17 November 2025).
23. Diaz, J.J.; Azar, F.K. Minimally invasive chest wall stabilization: A novel surgical approach to video-assisted rib plating (VARP). *Trauma Surg. Acute Care Open* **2019**, *4*, e000366. [CrossRef]
24. Riquet, M.; Hubsch, J.P.; Brière, J.; Debesse, B. Muscle-sparing posterolateral thoracotomy in children: Functional results. *Ann. Thorac. Surg.* **1990**, *50*, 934–939.
25. Elsharkawy, H.; Saifullah, T.; Kolli, S.; Drake, R. Rhomboid intercostal block. *Anaesthesia* **2016**, *71*, 856–857. [CrossRef]
26. Deng, W.; Hou, X.M.; Zhou, X.Y.; Zhou, Q.H. Rhomboid intercostal block combined with sub-serratus plane block versus rhomboid intercostal block for postoperative analgesia after video-assisted thoracoscopic surgery: A prospective randomized-controlled trial. *BMC Pulm. Med.* **2021**, *21*, 68. Erratum in *BMC Pulm. Med.* **2025**, *25*, 424. https://doi.org/10.1186/s12890-025-03601-4. [CrossRef]
27. Manici, M.; Salgın, B.; Söğüt, M.S.; Tanju, S.; Dilege, Ş.; Gürkan, Y.; Elsharkawy, H. Can Rhomboid Intercostal Block Be an Alternative to Paravertebral Block in Video-Assisted Thoracoscopic Surgery? A Randomized Prospective Study. *Diagnostics* **2024**, *14*, 2129. [CrossRef]